ELSEVIER

Journal of Hazardous Materials B:64 (1999) 263–281

Journal of Hazardous Materials

Temperature effect on ionic transport during soil electrokinetic treatment at constant pH

Fabienne Baraud *, Sylvaine Tellier, Michel Astruc

Laboratoire de Chimie Analytique, EP 132 CNRS, Université de Pau et des Pays de l'Adour, 64000 Pau, France

Received 9 April 1998; revised 20 July 1998; accepted 22 July 1998

Abstract

Laboratory experiments and theoretical modelling generally proposed for electrokinetic soil processing consider isothermal conditions at room temperature. Important increases of the soil temperature, due to the Joule effect, have been observed during pilot or field-scale tests. The temperature effect on the transport of ionic species present in the pore solution is investigated when an electric field is applied through the soil mass. Laboratory experiments are run at 20 and 40°C using kaolinite as soil model and one anion and one cation as model pollutants. An adapted methodology (pH control, steady state conditions) allows the measurement and the comparison of the ionic electrokinetic velocities at the two temperatures. Under the conditions developed, the temperature mainly influences the ionic velocities, which increase, for the two ions of interest, when the temperature rises.

Keywords: Electrokinetics; Kaolinite; Decontamination; Temperature; Velocity

1. Introduction

Numerous and various sources of soil contamination exist: waste disposal, polluting industrial activities (coal tar pits, mines tailing wastes…), excess of fertilisers, pesticides, as well as atmospheric deposition [1,2]. The polluted soil becomes a secondary pollution source, releasing toxic substances, that places human health and environmental surrounding at risk. The increasing demand for feasible and cost-effective remedial actions for soils have resulted in the development of alternative technologies, especially

* Corresponding author. Tel.: +33-05-59-92-30-90; fax: +33-05-59-02-93-77; e-mail: lca@messv2.univ-pau.fr

0304-3894/99/$ - see front matter
PII: S0304-3894(98)00190-3

in situ technologies. In situ treatments are preferred due to their lower costs and the elimination of human health risks during the excavation step, which is realised in most of the earlier remedial actions. Moreover, they cause less environmental disruption [3,4].

Electrokinetic remediation is emerging as one of the most promising in situ techniques. The method is based on the electrokinetic phenomena that occur when an electric field is applied to the saturated polluted soil by means of electrodes inserted in the soil mass. The pore fluid is used as the conductive medium [5]. This electric field induces a motion of the liquid and of the dissolved species that transports the contaminants to the electrodes from where they can be removed by adapted collection or separating processes (electrodeposition, chemical precipitation, ionic membranes...) [6,7].

The major advantages are: (a) a unique applicability to low permeability soils (clays, silts, till lenses and layers). Such soils have greater ability to adsorb pollutants, but are resistant to standard in situ remedial techniques, i.e., pump-and-treat methods which would require in this case a very high hydraulic gradient to be efficient [4,8]; (b) a high degree of control of flow direction, unlike soil flushing [2,3,9]; (c) the capability of removing a wide range of contaminants, especially heavy metals (unlike bioremediation, vapour extraction or soil incineration); and (d) a low electric power consumption.

Laboratory experiments have shown that it is possible to achieve high removal efficiencies by this method for various types of pollutants: heavy metals and inorganic species, such as As, Cr, Cd, Cu, Fe, Hg, Ni, Zn, NO_3^- [8,10–16], some radionuclides as uranium, thorium, strontium [7,17,18] as well as some organic compounds like phenol, toluene, ethanoic acid, benzene, *p*-nitrophenol... [3,19–21].

The transport processes are generated by the three major electrokinetic phenomena: electrophoresis, electromigration and electroosmosis.

Electrophoresis is the transport of charged particles (colloids, clay particles, organic particles...) under the influence of the electrical gradients. It should be of less importance in compacted systems, the solid phase being restrained from movement. Its significance only appears when pollutants are adsorbed on particles, when surfactants are introduced in the processing fluid to form micelles or when the technique is used for slurries [6,15].

Electromigration is the transport of charged species under the electrical field. The cations move towards the cathode, the anions towards the anode.

Electroosmosis is the movement of water through the soil matrix generated by the electric potential gradients.

Other possible transport mechanisms are hydraulic convection and ionic diffusion. Hydraulic convection can be neglected in the case of low permeability soils, the fluxes generated by the electrical driving forces being of much more importance [6,7,22]. Diffusion transport of ions can occur when concentration gradients exist or are produced by reactions between the various species present, by electrode reactions or any solid/liquid interface phenomena (sorption, precipitation, dissolution, complexation...) [23–25]. Soil surface properties (cation exchange capacity, adsorption capacity, sign and magnitude of the Zeta potential...) as well as speciation and dissolution of the pollutants are generally pH dependent [15]. Important variation of this parameter can be observed if not controlled: electrolysis of water being the dominant reaction at the

electrodes, H^+ and OH^- ions are produced, respectively, at the anode and at the cathode. These ionic species migrate through the soil, resulting in the development of an acid front from the anode towards the cathode and a basic one from the cathode towards the anode.

Application of the electric field for an extended period can result in several complications like variable conductivity values of the pore solution between anode and cathode and a sharp rise in pH near the cathode. Consequently, precipitation of dissolved species generally occurs in the cathodic basic region and a decreased or even a complete inhibited flow is observed [16,26]. Removal efficiency of transported ions can be drastically reduced.

Various conditioning techniques are now currently used to avoid such problems and enhance the process. Cathodic and/or anodic conditioning avoids the development of steep pH gradients, leads to regular solution conductivity and electrical gradients, resulting in higher removal efficiency [4,6,11,27]. Other techniques like selective membranes, CO_2 bubbling have been also proposed [11].

Temperature is also an important parameter that can influence the electrokinetic remediation process. During in situ treatment, the soil can be subject to external temperature fluctuations. Moreover, inherent to the process is the Joule effect. It corresponds to a partial conversion of the electrical energy into Joule heating, which finally results in energy lost for the ions transport and induces the increase of the soil temperature. In laboratory bench-scale experiments such effect is not observed: the electrical current (generally inferior to 5 mA cm^{-2}) and the experiment duration are low enough to neglect temperature effects [16]. However, Acar and Alshawabkeh [28] reported a rise of 10 to 20°C due to uncontrolled variations of electrical gradients. Very important temperature (till 40 to 50°C of increase) variations are more commonly observed on field-scale or pilot-scale studies [29–31]. Temperature can affect conductivities, ionic mobilities, electroosmosis and sorption reactions in a way that may enhance or delay the pollutants removal.

In the present work, we analyse the temperature effect on the contaminant transport during the electrokinetic treatment of soils at constant pH. Simplifying conditions are assumed. The influence of the hydraulic gradients is neglected as our study is restricted to low permeability clays. Diffusion is not included either, since considered a minor contributing component to the total flux [6]. Under such assumptions, the two major electrokinetic phenomena involved are electroosmosis and electromigration. Temperature effects on these two mechanisms and on the transport of anionic and cationic species are analysed. Laboratory experiments were performed at room temperature and at a higher regulated temperature on kaolinite, using a pore solution containing one anion and one cation as model contaminants. Theoretical and experimental results are compared.

2. Theoretical analysis

For simplicity the following assumptions are made. A mono-directional system, in which the laws governing the solutions apply, is considered. The electrical potential

gradient is constant with respect to time and space. Hydraulic and chemical gradients are of negligible influence compared to the electrical gradients (no diffusion nor advective flow). Moreover, the possible delaying reactions in the pore fluid (i.e. precipitation), or at the solid/liquid interface (i.e. adsorption) are neglected: the species are supposed to be dissolved in the liquid phase during the whole process.

Under such conditions, the major transport phenomena occurring during the application of an electric field on a low permeability soil are electromigration and electroosmosis [27]. The corresponding velocity of a species in the pore solution is then called the electrokinetic velocity [27].

The ionic species are moved by electromigration towards the electrodes (even in a stationary fluid). The direction of this migration depends on the charge of the ions (cations towards the cathode, anions towards the anode). The migration velocity (V_{em}^{i}) is directly proportional to the electric field applied ($\vec{E}$) and to the electrical mobility (u_i) of the species i of interest. In free solution this velocity is expressed by:

$$\vec{V}_{em}^{\,i} = u_i \vec{E}. \tag{1}$$

As the flow paths in soil are longer and more tortuous than in aqueous solution, the effective mobility in soil (u_i*) is related to its value in free solution by:

$$u_i* = u_i/\tau, \tag{2}$$

where τ is called the tortuosity factor [32,33]. Thus, the electromigration velocity of an ionic species i in a porous medium and a mono-directional system, can be expressed by:

$$\vec{V}_{em}^{\,i} = u_i* i_e \tag{3}$$

where: i_e, electrical potential gradient.

Electroosmosis is the movement of fluid due to the drag interaction between the bulk fluid of the liquid in the pore and a thin layer of charged fluid (the diffuse double layer) near the pore wall. As the natural solid surfaces are generally negatively charged. Therefore, the double layer is constituted of cationic species. Under the influence of the electric field, the mobile cations (in excess) exert more momentum to the pore fluid than anions do. Consequently, the resulting net electroosmotic flow observed is towards the cathode [4,7,33].

The electroosmotic flow rate (Q_{eos}) is described by the empirical relationship proposed by Casagrande [34]:

$$Q_{eos} = k_e S i_e \tag{4}$$

where S is the total cross-sectional area and k_e is called the coefficient of electroosmotic permeability (other parameters already defined).

The velocity of a fluid in a porous medium is defined by [35,36]:

$$V_{fluid} = Q_{fluid}/\theta S \tag{5}$$

The electroosmotic velocity (V_{eos}) towards the cathode can then be expressed by:

$$V_{eos} = \frac{Q_{eos}}{\theta S} = \frac{k_e}{\theta} i_e \tag{6}$$

where: θ, soil porosity, equivalent to water content in saturated conditions.

The velocity of an ionic pollutant (V_i) corresponds to the vectorial sum of the electromigration and electroosmotic velocities [5,37]. For a cationic species, the transport is enhanced as the both transport mechanisms cause the cation to migrate to the cathode. The velocity (towards the cathode) of a cationic species i is then given by:

$$V_i = \left(u_i* + \frac{K_e}{\theta} \right) i_e = u_i* + \frac{Q_{eos}}{\theta S}. \quad (7)$$

Anionic species are drawn towards the anode by electromigration. Their migration is then decreased by the opposite electroosmotic flow. The velocity (towards the anode) of an anionic species j is then given by:

$$V_j = \left(u_j* - \frac{k_e}{\theta} \right) i_e = u_j* - \frac{Q_{eos}}{\theta S}. \quad (8)$$

For non-ionic species there is no electromigration transport. These species are only moved by electroosmotic advection. The direction and the velocity of their migration correspond to those of the electroosmotic flow. Expressions (7) and (8) have been experimentally validated in our previous work for various cationic species (Na^+, K^+, Ca^{2+}) at room temperature [27].

Let us consider now the influence of temperature on the transport and velocity of the pollutant species during the electrokinetic treatment.

Temperature changes during electrokinetic treatment are generally due to the Joule effect, whose magnitude is directly proportional to the electrical current (I) and the resistance of the medium (Ω). Joule heat P is defined by [38]:

$$P = I^2\Omega = i_e^2 \kappa S \quad (9)$$

where: κ, conductivity of the solution.

The largest increases of temperature during electrokinetic remediation processing have been reported for pilot or field-scale experiments [29,31]. The temperature could have an influence on the electrical mobility [39] as well as on the electroosmotic flow [40].

2.1. Electromigration

The electrical mobility u_i of a specified species i is defined by [41]:

$$u_i = \frac{z_i e_o}{6\pi\eta r_i} \quad (10)$$

where: z_i, charge of the species; e_o, elementary charge; η, viscosity; r_i, Stoke radius.

The primary effect of temperature is through the change of viscosity. Viscosity variations affect all ions in the same way. Temperature-induced changes of viscosity are frequently approximated as 2% per °C [39,41,42]. Then:

$$u_i*(T) = u_i*(T_o)\left[1 + 0.02(T - T_o)\right] \quad (11)$$

where: T, T_o, temperature.

This leads finally to an increase of 2% per °C of the electromigration velocity (from Eqs. (3) and (11)), as temperature has no influence on the value of the imposed electric field. Then:

$$V_{em}^{i}(T) = V_{em}^{i}(T_o)\left[1 + 0.02(T - T_o)\right]. \tag{12}$$

2.2. Electroosmosis

The temperature influence on the electroosmotic flow (and velocity) is not so well known. Some authors report that this flow increases with temperature [40]. But this variation is not so easy to quantify, as many simultaneous parameters influence the phenomenon.

The Helmholtz–Smoluchwski theory is the most widely used theory to describe electroosmosis from a microscopic point of view. The electroosmotic permeability coefficient is then described by:

$$k_e = \frac{\varepsilon \xi \theta}{4\pi\eta}, \tag{13}$$

where ϵ is the dielectric constant of the solution that decreases when the temperature increases. η is the solution's viscosity, that also depends on the temperature value. Generally η decreases when the temperature rises, but the relationship can be affected by the nature and the composition of the solution.

ϵ is the electrokinetic potential, that can be described by [39]:

$$\xi = \frac{\lambda_D \sigma}{\varepsilon} \tag{14}$$

where σ represents the surface charge. λ_D is double layer thickness, assimilated to the Debye length, which varies with T according to:

$$\lambda_D = \sqrt{\frac{\varepsilon RT}{2C_e z^2 F^2}}\ . \tag{15}$$

where: F, Faraday's constant; C_e, electrolyte concentration. Thus, ϵ also varies with the temperature.

The relationships between the temperature and each of these parameters are not all well defined. Consequently, the temperature effect on the electroosmosis cannot be precisely theoretically predicted.

From this first approach, it appears that a temperature rise should increase the ionic electromigration velocity and the electroosmotic flow (according to some experimental observations [40,41]). Then the cationic species should be greatly enhanced as the two phenomena are additive. But the delaying or enhancing influence of temperature on anions transport will depend on the ratio of the variation of each of the two terms.

3. Experimental

Experiments were run on kaolinite as soil model. This non swelling clay is often chosen for electrokinetic experiments because of its low activity and its relatively high electroosmotic water transport efficiency. One cation (Na^+) and one anion ($Cr_2O_7^{2-}$) were used as ionic contaminant models (electrical mobility: 45.10^{-5} and 47.10^{-5} cm^2 s^{-1} V^{-1}, respectively, at 18°C [43]). These ions were chosen so as to remain as free ionic species, i.e. to avoid any undesired reactions (precipitation, complexation) within the pore solution for the working pH range [44].

The experimental apparatus is represented in Fig. 1. It consists of an horizontal PVC cell. The saturated sample is confined in the central part, separated from the two end chambers by filters of polyamide fibbers. A direct power supply provides a constant voltage between the platinum wires electrodes immersed in each end chamber solution. Respective conditioning fluids are continuously supplied by peristaltic pumps. An alkaline solution (ethanoate solution) is introduced at the anode to neutralise the H^+ ions produced by the electrolysis of water. Moreover, it assures a continuous supply of solution that avoids soil dewatering and electroosmotic flow cessation. At the cathode, an acidic solution (ethanoic acid) neutralises the OH^- ions produced by the electrolysis of water. An ethanoic buffer is thus produced within the cell. This procedure results in a regular pH profile in the sample and a linear distribution of electrical gradients as suggested by our previous laboratory experiments [18], [27]. Ethanoic buffer ($pK_a = 4.8$) was chosen for next actual situations in mind as it is a cheap, non toxic and biodegradable reagent.

Overflow systems permit collection of the effluents. Measurements of the electrical gradients, current density, pH (by inserting directly a combination pH electrode in the sample, voltage being stopped during the measurements), volumetric flow rates and chemical composition of the influents and effluents are carried out during the experiments. Concentrations of sodium cations are determined with a Corning Flame photometer 410 and dichromate anions by atomic absorption spectrometry with a IL 451 AA Flame spectrometer.

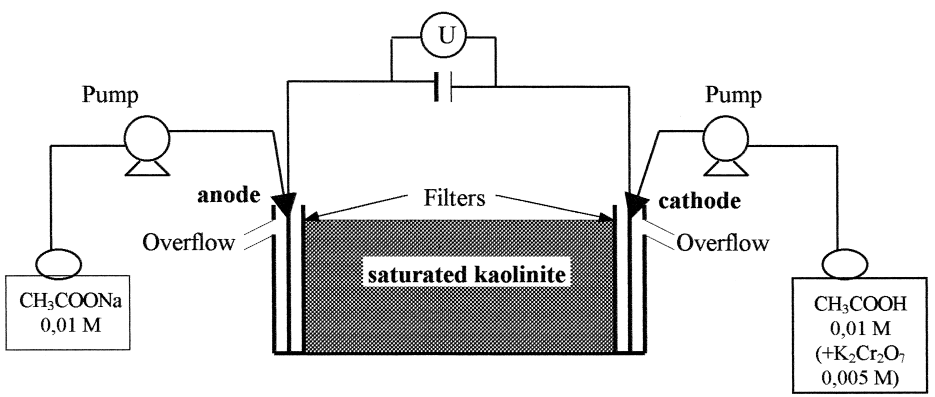

Fig. 1. Laboratory test cell. *U*: power supply (50 V imposed). cell dimensions: 50 cm × 4 cm × 4 cm.

The sample is prepared by mixing 500 g of commercial kaolinite (extra pure, low bacteria content, Merck) with 400 ml of ethanoate buffer solution, 10^{-2} mol l^{-1} ($CH_3COONa + CH_3COOH$). This corresponds to a porosity value of 0.672 and a theoretical tortuosity of 1.24 [27].

A constant voltage of 50 V is applied across the cell to get a theoretical gradient of 1 V cm^{-1}. The first part of experiment is a conditioning period, which is realised in order to saturate the kaolinite with Na^+ ions (Na-kaolinite is then obtained), by introducing sodium ethanoate solution at the anode and ethanoic acid solution at the cathode (both, concentration of 10^{-2} mol l^{-1} and flow rate of 30 ml h^{-1}), until steady state conditions are obtained.

Dichromate anions are then additionally introduced at the cathode by dissolving $K_2Cr_2O_7$ in the ethanoic acid solution, to get a concentration of 5.10^{-3} mol l^{-1} of $Cr_2O_7^{2-}$, and a new steady state condition.

Two different experiments were initiated for the conditioning step at room temperature (20 ± 1°C). The temperature (T) remains unchanged at the introduction of dichromate ions for one of the run (exp1), whereas an external temperature of 40°C is imposed for the second one (exp2), by immersing the cell in a thermostatic sand bath till the end of the run.

The two runs are stopped simultaneously. The kaolinite sample is then divided in 12 sections, each of it being centrifuged for 15 min (4000 rpm). The supernatant (the pore solution) is analysed for the ions of interest, pH and conductivity. The remaining kaolinite is dried for 16 h at 105°C to determine the final water content (humidity percent) by weight comparison.

4. Results

This methodology has already proven its feasibility to get regular pH and electrical gradient profiles [18]. A good control of the phenomena is achieved, i.e. electroosmosis and electromigration are then the dominant mechanisms (under steady state conditions) [27]. Under such conditions, the experimental velocity V_{exp} has been shown to correspond to the electrokinetic velocity V_i, that can be calculated from Eqs. (7) and (8), respectively, for the cationic and anionic species [27]. The experimental velocity is calculated as followed:

$$V_{exp} = J_i/\theta C_i = Q_i/\theta C_i S \tag{16}$$

where: J_i, molar flux; Q_i, molar flow rate; S, cross-sectional area; C_i, concentration in the pore solution.

4.1. pH and electrical gradients

A regular pH profile is achieved throughout the sample for the two experiments (values closed to the pK_a value of ethanoate buffer solution) (Fig. 2). The methodology

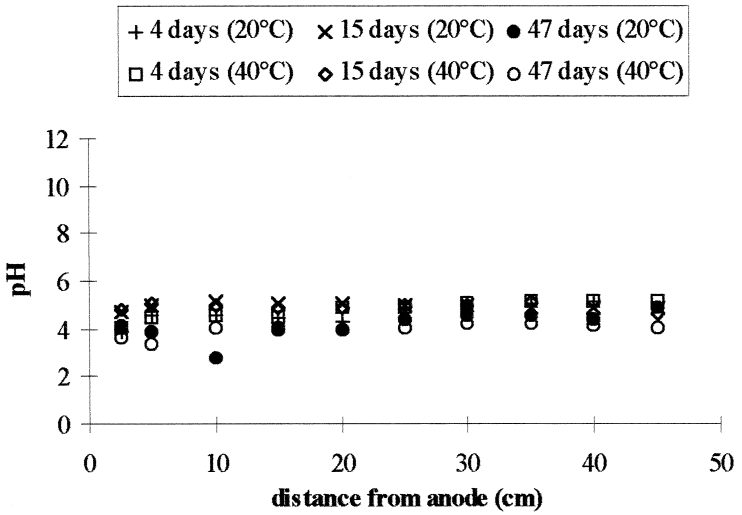

Fig. 2. pH profiles in the kaolinite sample (exp1; exp2).

developed is efficient to control the pH during the treatment at the two temperatures. Temperature does not affect the pH distribution, neither the pH value established all along the sample.

Regular profiles of the electrical gradient are established for the two runs all along the sample and at any time of the run. An average value of 1 V cm^{-1} is maintained (Fig. 3a,b).

4.2. Moisture content

For the two runs, the final moisture content in the sample remains close to the value initially imposed (45%) (Fig. 4). This indicates that the sample remains saturated during the whole experiment (with a corresponding porosity of 0.672) at any time of the run for the two temperatures studied.

4.3. Pore solution concentrations

Under the specific conditions used (kaolinite, Na^+ and $Cr_2O_7^{2-}$ as model contaminants), the final concentration are not significantly influenced by the temperature value in the temperature range studied (other experimental conditions being identical). The average concentrations in the pore solution are, respectively, at room temperature and 40°C: $(8.0 \pm 0.1)10^{-3}$ and $(7.1 \pm 0.1)10^{-3}$ mol l^{-1} for Na^+ ions; $(2.9 \pm 0.2)10^{-3}$ and $(2.4 \pm 0.2)10^{-3}$ mol l^{-1} for the $Cr_2O_7^{2-}$ ions. As the porosity remains constant and the concentrations are nearly the same at the two temperatures studied, the ionic transport will mainly be affected by the velocity variation, as the velocity (V_i) is related to the ionic flux (J_i) and concentration (C_i) according to Eq. (16).

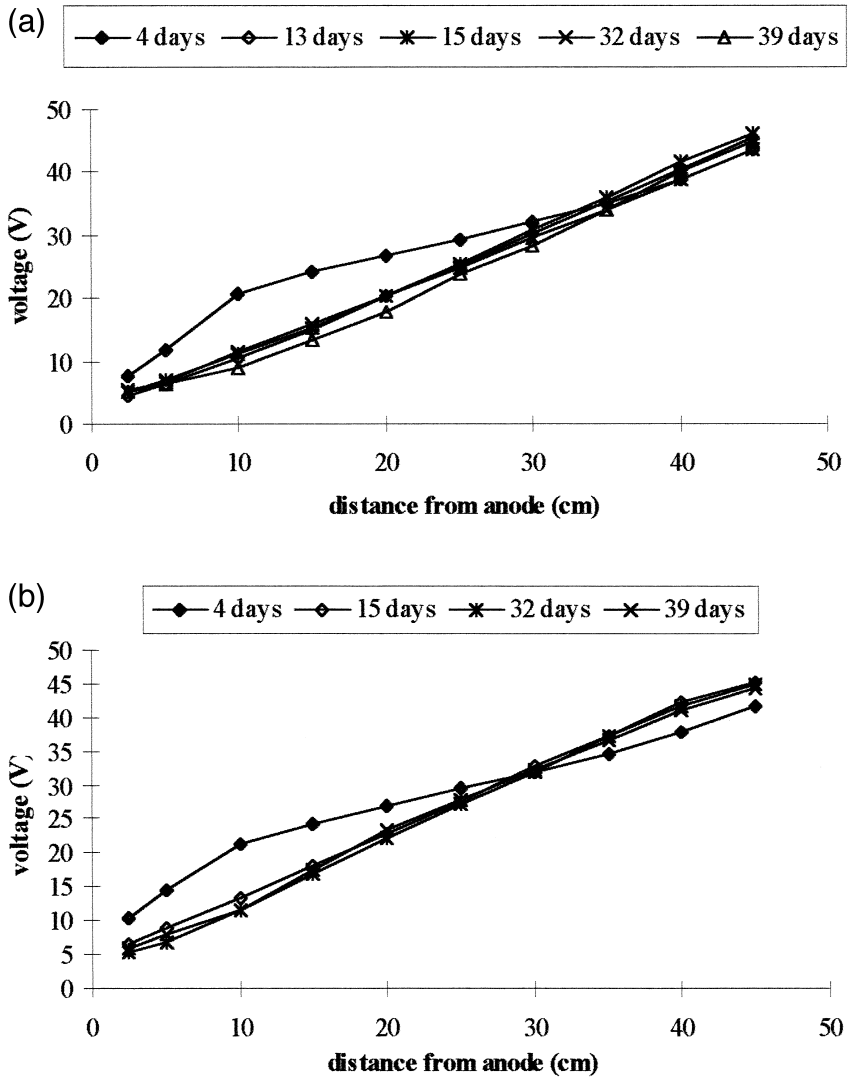

Fig. 3. (a) Electrical gradients in the kaolinite sample (exp1). (b) Electrical gradients in the kaolinite sample (exp2).

4.4. Electroosmosis

Electroosmotic flow rate is determined by volume comparison of injected solutions and collected effluents at the two ends of the cell (respectively called anodic and cathodic electroosmosis) [27]. Fig. 5a and b represent the cumulative volumes (V_{cum}) of pore solution transported by electroosmosis vs. time (t). Linear regressions calculated for each step of the runs (unchanged conditions) indicate that the various curves

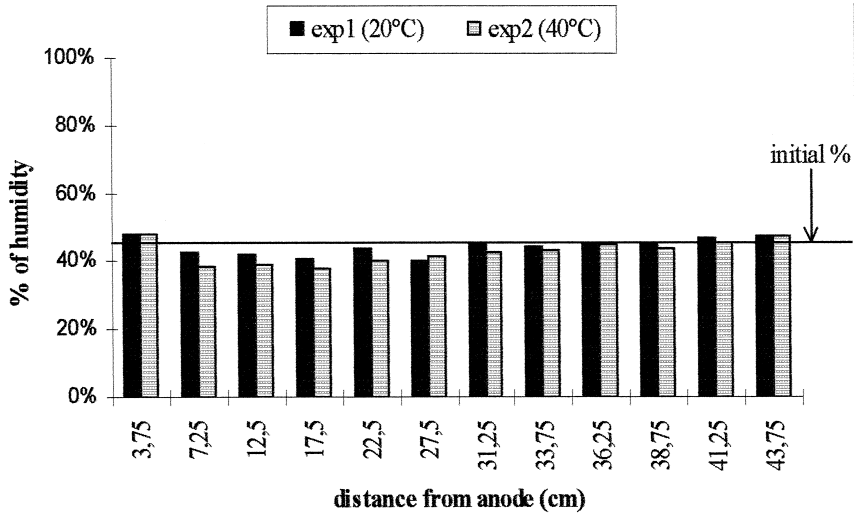

Fig. 4. Final percentage of humidity in the kaolinite sample (exp1; exp2).

$V_{cum} = f(t)$ obtained can actually be assimilated to linear function of time. The corresponding slopes (α) correspond to the average values of the electroosmotic flow rate (Table 1).

Some differences are noticed between anodic and cathodic measurements (Table 1, Fig. 5a,b). They are attributed to water evaporation during its transport towards the cathode by electroomosis, as the working cell is an open system (to be closest as possible to field conditions).

A significant variation of electroosmotic flow rates appears from 20 to 40°C: electroosmosis increases with the temperature, as some authors reported [40]. This variation is higher at the anode (+58%, corresponding to a flow rate increase around 2.9% per °C) than at the cathode (+24%, corresponding to +1.3% per °C). It may be explained by a more important water loss at higher temperature between the cathodic and anodic regions.

4.5. Current

The current density j is related to the ionic fluxes according to

$$\vec{j} = F \sum z_i \vec{J_i}. \tag{17}$$

The electrical intensity I (experimental measurement) is expressed by

$$I = j/S. \tag{18}$$

From Eqs. (16)–(18), it can then be written:

$$I = F \sum z_i \theta C_i V_i. \tag{19}$$

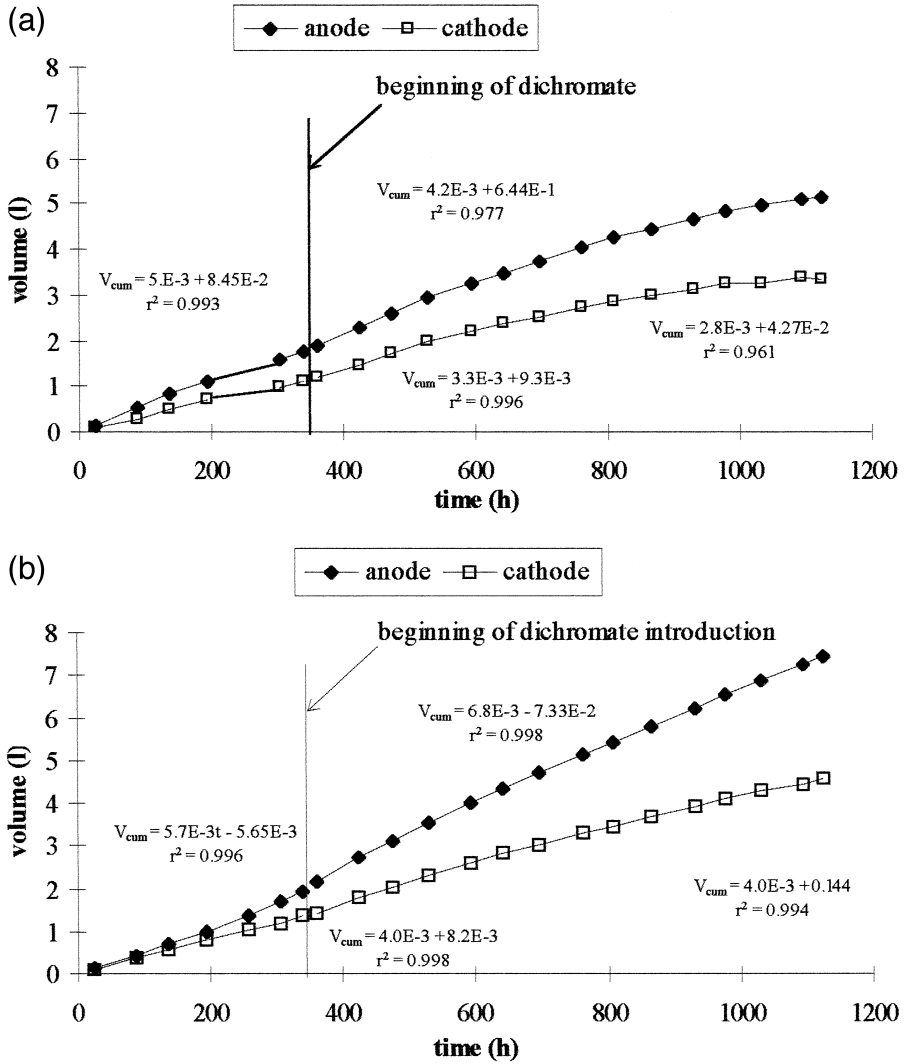

Fig. 5. (a) $V_{cum} = f(t)$ (exp1). (b) $V_{cum} = f(t)$ (exp2).

For each step of a run, a constant value of I is established under steady-state conditions, corresponding to constant values of ionic fluxes (Figs. 6 and 7). The transference numbers (t_i) were calculated for the two ions of interest, as

$$t_i = \frac{u_i * C_i}{\sum u_k * C_k}. \tag{20}$$

It appears that I is mainly depending on the sodium flux (average values corresponding to stationary conditions are, respectively, for the sodium and dichromate ions: $t^+_{Na} = 0{,}66$

Table 1
Electroosmotic flow rates

No.		Anode			Cathode		
		Q_{eos}^{exp}	α	r^2	Q_{eos}^{exp}	α	r^2
1	1st step	5.7	5.0	0.99	3.6	3.3	1.00
	2nd step	4.5	4.2	0.98	3.2	2.8	0.96
2	1st step	5.9	5.7	1.00	4.1	4.0	0.99
	2nd step	7.1	6.8	1.00	4.0	4.0	0.99

Q_{eos}^{exp}: Experimental electroosmotic flow rate ($cm^3\ h^{-1}$).
α: Slope of the linear regression or theoretical electroosmic flow rate ($cm^3\ h^{-1}$).

and $t_{Cr_2O_7^{2-}} = 0.32$), as suggested by Fig. 7 which compares the measured intensity and the flow rates (eq/h) of each species. Under such conditions, it appears that the transference number of the ethanoate ions, simultaneously present in the pore solution, is very low (around 0.02). This indicates that these anions do not contribute significantly to the current conduction, partly due to their lower electrical mobility (35.10^{-5} $cm^2\ s^{-1}\ V^{-1}$ at 18°C [43]) compared to sodium and dichromate ions, but also to the fact that they undergo the weak acid/base equilibrium with ethanoic acid, which is an non-ionic species.

4.6. Ionic transport

According to previous work [27], prediction of the theoretical expression (7) compare very well with the experimental velocity results (V_{exp}) for the sodium cation at room temperature (Table 2). A good agreement between experimental and theoretical values is

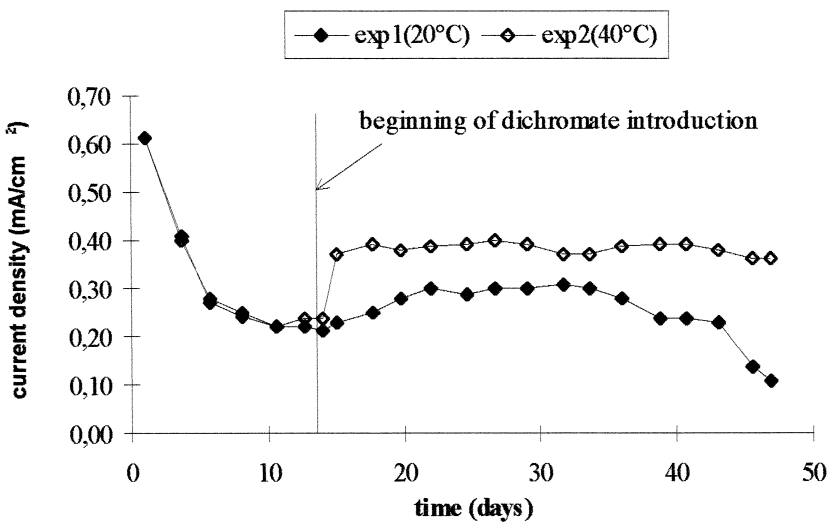

Fig. 6. Current densities during the experiments (exp1; exp2).

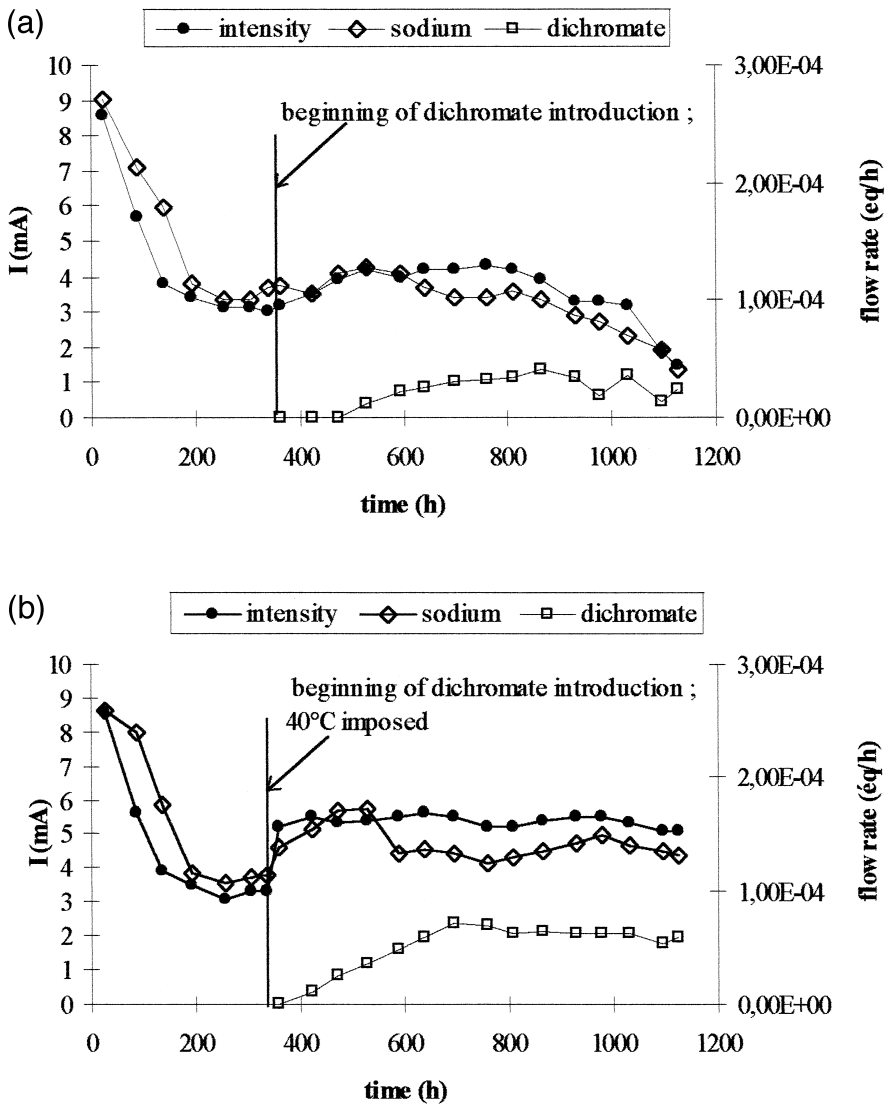

Fig. 7. (a) Electrical intensity and molar flow rates (exp1). (b) Electrical intensity and molar flow rates (exp2).

obtained also for the dichromate anion. Furthermore, this is also verified, for these two ions, at 40°C (Table 2). Electromigration and electroosmosis remain the major transport phenomena at this higher temperature and Eqs. (7) and (8) can actually predict the electrokinetic velocities of any ions, under specific conditions, using corresponding values of electrical mobilities and electroosmosis at 40°C.

To set free of the influence of the experimental electrical gradient value (that is used to calculate V_i [27]), the temperature effect on the velocity will be determined by

Table 2
Velocities results

No.	Ion	Anode			Cathode		
		V_i	V_i'	V_{exp}	V_i	V_i'	V_{exp}
1 (20°C)	Na^+ $Cr_2O_7^{2-}$	13	52	15	14	41	14
		6	15	8	15	26	23
2 (40°C)	Na^+ $Cr_2O_7^{2-}$	47	65	45	34	61	45
		17	24	16	18	32	20

V_i: electrokinetic velocity (cm day^{-1}).
V_i': electrokinetic velocity for an electrical gradient of 1 V cm^{-1} (cm day^{-1}).
V_{exp}: experimental velocity (cm day^{-1}).

comparison of V_i' (Table 2), which corresponds to the electrokinetic velocity for a standard electrical gradient of 1 V cm^{-1}.

4.6.1. Sodium transport

For the two experiments the conditioning step is run under the same conditions (i.e. room temperature). Identical sodium flow rates are then observed (Fig. 8), which shows the reproducibility of such experiments. The temperature effect is analysed on the second part of the runs. Input and output molar flow rates are enhanced by the temperature rise (exp2), as a combined effect of the increase of the electrical mobility (then electromigration) and electroosmotic flow rate as predicted. A corresponding increase of the sodium velocity is observed, which corresponds to a rise of 1 cm day^{-1} per °C (Table 2).

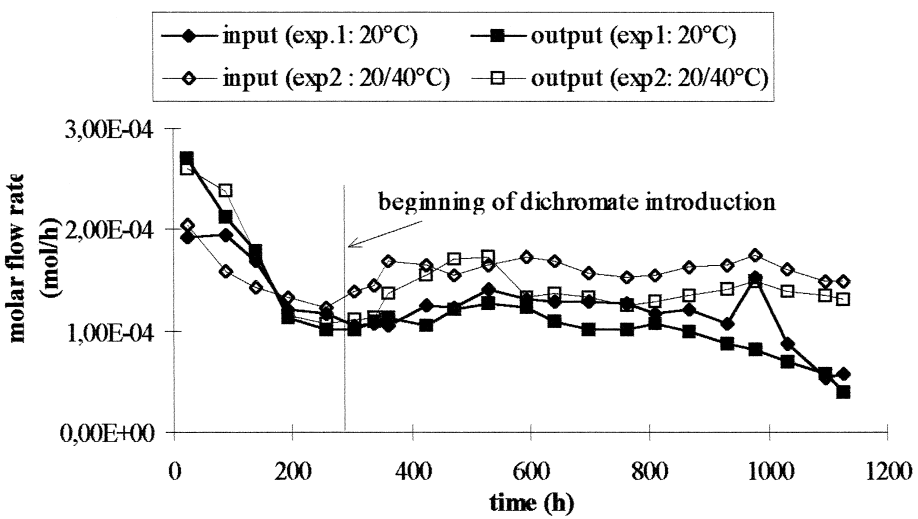

Fig. 8. Sodium molar flow rates (exp1; exp2).

4.6.2. Dichromate transport

The dichromate flow rate value is depending on the relative magnitude of the electromigration transport and the opposite delaying electroosmotic flow (cf. Eq. (8)). Quite similar input and output flow rates are observed for the two temperatures studied (Fig. 9). Input flow rate is higher at 20°C than at 40°C, whereas output flow rates are the same at the two temperatures.

The electroosmosis increase does not seem to be high enough (proportionally to the electromigration rise) to totally prevent the dichromate anions from migrating towards the anode. But it appears to be sufficient to delay dichromate entrance (at the cathode) to obtain lower values of input flow rate at 40°C. In the anodic region, the temperature is slightly higher. Then, the increase of the electromigration transport exactly compensate the electroosmosis rise at 40°C, resulting in no significant variation of the output flow rate between the two temperatures.

More generally, according to our previous work [27,44], the relative contribution of electroosmosis to the total transport represents a maximum of 25% (75% for electromigration).The electromigration and the electroosmosis variations with T are, respectively, 2% per °C and around 3% per °C (maximum variation observed).

For an anionic species, the variation of the electrokinetic velocity with the temperature rise is then: +1.5% per °C, due to the electromigration increase and −0.08% per °C, due to the electroosmosis increase. Under such conditions, the electrokinetic velocity of any anionic species increases when the temperature rise.

A temperature influence on the dichromate velocity, less important than for the cationic species, is then finally observed, as an increase of V_i' is noted (Table 2).

The differences noticed for the V_i values are correlated to the various measured electrical gradient that have been lower by some experimental problems at the end of the runs.

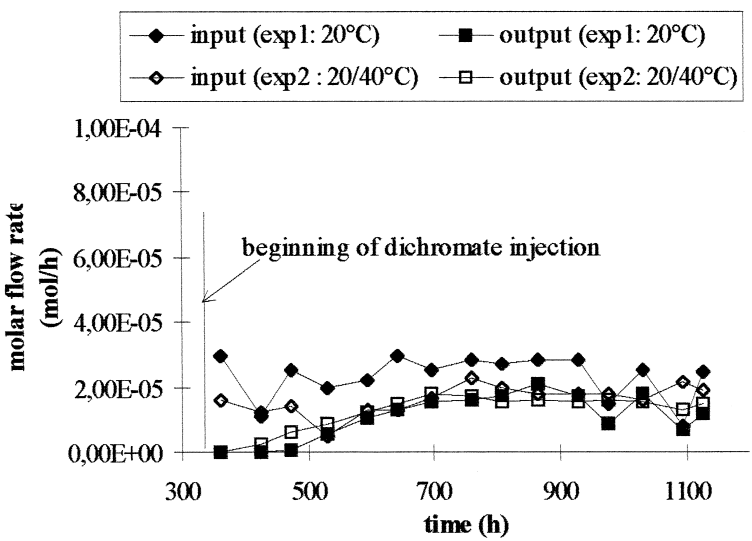

Fig. 9. Dichromate flow rates (exp1; exp2).

4.6.3. Consequences

Under the developed conditions, the temperature rise enhances the cationic transport, as predicted, as well as the anionic one, for the specific anion studied.

As a consequence, the time necessary for a species to move from one point to another would be reduced. Then the treatment time and associated costs (especially, power consumption $\boldsymbol{P}$, as

$$\boldsymbol{P} = \int_{o}^{t} UI\,\mathrm{d}t \tag{21}$$

where: U, voltage, could be minimised.

Alternatively, an increase of the electrical current I (when working under constant voltage) results from the transport acceleration (Fig. 6) as I is related to the ionic fluxes, according to Eq. (17). This induces a rise of the power consumption (and associated costs).

In the developed conditions (without any consideration of possible energy losses), the sodium or the dichromate ions cross the kaolinite sample with a corresponding power consumption that remains the same at the two temperature studied (7.6 and 23 kW h m^{-3}, respectively). This can be correlated to the fact that the temperature only influence the ionic fluxes through its effect on the electrokinetic velocity, the concentrations in the pore solution being similar at the two temperatures. The time gain at 40°C, due to the velocity increase, compensates the current increase.

During a real decontamination process, the dissolved species are transported with their electrokinetic velocity [27], but the concentrations in the pore solution depend on sorption phenomena. In such a case, the temperature influences the ionic fluxes by its effects on the electrokinetic velocity (as previously presented) as well as on the desorption process (to be determined). Therefore, the temperature influence on the power consumption should differ from the above laboratory case.

5. Summary and conclusions

This work studies the temperature influence on an electrokinetic soil processing, when electromigration and electroosmosis are the two main phenomena. The temperature range studied corresponds to temperature variations actually observed during electrokinetic treatment in pilot-scale or field-scale tests.

A simplified theoretical analysis predicted a simultaneous increase of electromigration and electroosmosis with the temperature. As these two mechanisms are additive for the cationic transport, cationic species removal should then be enhanced by a temperature rise. For anionic species, the temperature effect would depend on the relative contribution of each mechanisms, as anions are delayed by the opposite electroosmotic flow.

Experiments were carried out at two temperatures (room temperature and 40°C), with kaolinite as soil model and one anion and one cation as model pollutants. The developed methodology, with a successful control of pH, allowed a good control of the phenom-

ena: electromigration and electroosmosis are the major phenomena arising during the treatment. The developed expressions (7) and (8) for the electrokinetic velocity remain validated for cationic and anionic species at the two temperature studied. Under the developed conditions, no significant temperature influence is observed for pH, humidity and pore solution composition. The temperature rise enhances the cationic transport as well as the anionic movement, which indicates that electromigration proportionally remains the dominant transport mechanism of the anionic movement. The electrokinetic velocities increase with the temperature. This could then constitute an advantage as the pollutant removal is accelerated, which would reduce the necessary treatment time and corresponding costs. But, a higher temperature also results in a higher current density.

Finally, the temperature rise could be beneficial for electrokinetic soil processing if the processing time reduction at least compensated the energy lost generated. For the two experiments presented, as the concentrations in the pore solution are not affected by the temperature, the power consumption remains unchanged.

References

[1] A. Bermond, Analusis Magazine 22 (2) (1994) M8.
[2] Z. Li, J.W. Yu, L. Neretnieks, Journal of Contaminant Hydrology 22 (1996) 241.
[3] S.V. Ho, P.W. Sheridan, C.J. Athmer, M.A. Heitkamp, J.M. Brackin, D. Weber, P.H. Brodsky, Environ. Sci. Technol. 29 (1995) 2528.
[4] Y.S. Choi, R. Lui, Journal of Hazardous Materials 44 (1995) 61.
[5] Y.B. Acar, E.E. Ozsu, A.N. Alshawabkeh, M.F. Rabbi, R.J. Gale, Chemtech, 1996, p. 40.
[6] Y.B. Acar, A.N. Alshawabkeh, Environ. Sci. Technol. 27 (13) (1993) 2638.
[7] A. Ugaz, S. Puppala, R.J. Gale, Y.B. Acar, Chem. Eng. Comm. 129 (1994) 183.
[8] B.E. Reed, M.T. Berg, J.C. Thomson, J.H. Hatfield, Journal of Environmental Engineering 121 (11) (1995) 805.
[9] J.M. Dzenetis, Environ. Sci. Technol. 31 (1997) 1191.
[10] C.D. Cox, M.A. Shoesmith, M.M. Ghosh, Environ. Sci. Technol. 30 (1996) 1933.
[11] R.E. Hicks, S. Tondorf, Environ. Sci. Technol. 28 (1994) 2203.
[12] J.B. Jensen, V. Kubes, M. Kubial, Environmental Technology 15 (1994) 1077.
[13] J. Larrañaga, Doctoral thesis no. 309, Pau, France, 1996.
[14] I. Le Hecho, Doctoral thesis no. 264, Pau, France, 1996.
[15] S. Pamukcu, J.K. Wittle, Environmental Progress 11 (3) (1992) 241.
[16] Y.B. Acar, J.T. Hamed, A.N. Alshawabkeh, R.J. Gale, Géotechnique 44 (2) (1994) 239.
[17] S. Pamukcu, J.K. Wittle, in: 14th Annual US Department of Energy Low-level Radioactive Waste Management Conference Proceedings, 1993, pp. 256–278.
[18] M.C. Fourcade, Doctoral thesis no. 315, Pau, France, 1996.
[19] B.A. Segall, C.J. Bruell, Journal of Environmental Engineering 118 (1) (1992) 84.
[20] C.J. Bruell, B.A. Segall, M.T. Walsh, Journal of Environmental Engineering 118 (1) (1992) 68.
[21] Y.B. Acar, ASCE Speciality Conference, Ground Improvement and Grouting, 1992, pp. 1–25.
[22] N.C. Lockhart, Colloids and Surfaces 6 (1983) 239.
[23] D.J. Wilson, Separation Science and Technology 31 (4) (1996) 435.
[24] D.J. Wilson, J.M. Rodriguez-Maroto, C. Gomez-Lahoz, Separation Science and Technology 30 (15) (1995) 2937.
[25] D.J. Wilson, J.M. Rodriguez-Maroto, C. Gomez-Lahoz, Separation Science and Technology 30 (16) (1995) 3111.
[26] S. Thevanayagam, J. Wang, in: International Congress on Environmental Geotechnics, Thomas Telford, London, 1994, pp. 379–385.

[27] F. Baraud, S. Tellier, M. Astruc, Journal of Hazardous Materials 56 (1997) 315.
[28] Y.B. Acar, A.N. Alshawabkeh, Journal of Geotechnical Engineering 122 (3) (1996) 173.
[29] R. Lageman, W. Pool, G. Seffinga, Chemistry and Industry, September, 1989, p. 585.
[30] R. Lageman, Environ. Sci. Technol. 27 (13) (1993) 2648.
[31] N. Costarramone, Doctoral thesis no. 350, Pau, France, 1996.
[32] C.D. Schakelford, Journal of Contaminant Hydrology 7 (1988) 177.
[33] A.T. Yeung, S. Dalta, Can. Geotech. J. 32 (1995) 569.
[34] L. Casagrande, Géotechnique 1 (3) (1949) 159.
[35] G. De Marsily, Hydogéologie Quantitative, Masson édns., Paris, 1981.
[36] J.P. Brun, Procédés de séparation par membranes, Masson édns., Paris, 1989.
[37] Y.B. Acar, M.F. Rabbi, E.E. Ozsu, Journal of Geotechnica and Geoenvironmental Engineering 123 (3) (1997) 239.
[38] J.P. Longchamp, Comprendre et appliquer l'électrocinétique, Masson édns., Paris, 1989.
[39] P. Gareil, Analusis 18 (1990) 221.
[40] M. Bonnemay, J. Royon, Techniques de l'ingénieur, 1974, D912-1.
[41] R. Khun, S. Hoffstetter-Khun, Capillary Electrophoresis: Principles and Practice, Springler-Verlag, 1993.
[42] P. Jandik, G. Bonn, Capillary Electrophoresis of Small Molecules and Ions, VCH Publishers, New York, 1993.
[43] G. Milazzo, Electrochemistry. Theoretical principles and practical applications, Elsevier, Netherlands, 1963.
[44] F. Baraud, Doctoral thesis no. 398, Pau, France, 1997.